

## Self-consistent polaron scattering rates in quasi-one-dimensional structures

S. Briggs, B. A. Mason,\* and J. P. Leburton

*Beckman Institute for Advanced Science and Technology and Department of Electrical and Computer Engineering,  
University of Illinois at Urbana-Champaign, Urbana, Illinois 61801*

(Received 22 August 1989)

We calculate the polaron self-energy in quantum-wire structures. We use the Fock approximation and consider the interaction of electrons and polar optic phonons in GaAs wires of different sizes at 300 K and solve for the self-energy iteratively. The result  $\Sigma(E, k)$  is presented as a function of both  $E$  and  $k$ . We compare  $\text{Im}\Sigma$  with a simple first-order calculation using Fermi's "golden rule" to investigate the importance of higher-order quantum effects. A constant broadening of the density of states has been included in Fermi's "golden rule" and is successful in reproducing the correct scattering rate.

The investigation of quasi-one-dimensional (quasi-1D) artificial structures is a rapidly growing field chiefly stimulated by the considerable advances in the fabrication of highly confined electronic systems. New quantum phenomena have been observed at temperatures above 4.2 K.<sup>1</sup> With these new developments, transport with dissipation<sup>2</sup> and electron-phonon interaction is a subject of recent attention. In III-V compounds, high-energy transport is essentially limited by interactions with polar optic phonons (POP's).

In general, phonon scattering rates in transport simulations are computed according to Fermi's "golden rule"<sup>3</sup>

$$W(\mathbf{k}_i, \mathbf{k}_f) = \frac{2\pi}{\hbar} |M(\mathbf{k}_i, \mathbf{k}_f)|^2 \delta_{\mathbf{k}_i - \mathbf{k}_f \pm \mathbf{q}} \times \delta(E(\mathbf{k}_i) - E(\mathbf{k}_f) \pm \hbar\omega), \quad (1)$$

where  $W(\mathbf{k}_i, \mathbf{k}_f)$  is the transition probability from an initial electron state  $\mathbf{k}_i$  to a final state  $\mathbf{k}_f$ ,  $M(\mathbf{k}_i, \mathbf{k}_f)$  is the corresponding matrix element for the transition,  $E(\mathbf{k}_i)$  is the initial electron energy,  $E(\mathbf{k}_f)$  is the final electron energy,  $\mathbf{q}$  is the phonon wave vector, and  $\hbar\omega$  is the phonon energy. Fermi's "golden rule" is only valid if the scattering rate is low enough so that the scattering events are spatially and temporally independent.  $W(\mathbf{k}_i, \mathbf{k}_f)$  is then integrated over all final states to obtain the total scattering rate as a function of the initial electron energy. This introduces a density of states term  $D(E_i \pm \hbar\omega)$ ,

$$D(E_i \pm \hbar\omega) = \frac{1}{\hbar} \left( \frac{m^*}{2(E_i \pm \hbar\omega)} \right)^{1/2} \quad (2)$$

with  $m^*$  the effective mass. The functional dependence of  $D(E)$  is a consequence of the semiclassical expression of energy conservation which ignores any quantum correlations between scattering events. Clearly, this term diverges for  $E(\mathbf{k}_i) = \hbar\omega$ .

A more accurate description of the electron-phonon interaction considers the self-energy  $\Sigma(k, E)$  which can be calculated using the Fock approximation.<sup>4</sup> This approximation is a general method which includes higher-order quantum effects (including collisional broadening) in the

electron-phonon interaction. In 3D calculations the strong  $q$  dependence of the matrix element makes a self-consistent treatment of POP's difficult;<sup>5</sup> however, the slowly varying  $q$  dependence in 1D systems make the problem tractable.

In this Rapid Communication, we include the correct  $q$  dependence in the matrix element and employ an iterative method to solve the Fock approximation self-consistently. This approach gives the full  $k$  and  $E$  dependence of the self-energy  $\Sigma$  exactly. We perform this calculation for several different sized GaAs quantum-wire structures where the confinement is due to an infinite square well in one direction and a semi-infinite triangular potential in the other direction. The calculation is performed at 300 K and considers a single subband with inelastic POP scattering. We then compare our results for  $\text{Im}\Sigma$  with the rates obtained from Fermi's "golden rule."

In 1D systems, the Fock approximation for the self-energy  $\Sigma$  is given by

$$\Sigma(k, E) = \int \frac{dq}{2\pi} \frac{g_e^2(k-q)}{E - \hbar\omega - \varepsilon(q) - \Sigma(q, E - \hbar\omega)} + \int \frac{dq}{2\pi} \frac{g_a^2(k-q)}{E + \hbar\omega - \varepsilon(q) - \Sigma(q, E + \hbar\omega)}, \quad (3)$$

where  $g_e^2$  and  $g_a^2$  are the electron-phonon coupling constants corresponding to emission and absorption processes which include the 1D form factors.  $k$  and  $q$  are scalars corresponding to the components of the electron and phonon wave vectors parallel to the wire, and  $\varepsilon$  is the electron dispersion relationship (assuming the effective-mass approximation). This equation is then solved self-consistently for  $\Sigma$ .

Because of the divergence in the denominator of Eq. (3), brute-force integrations (which must be done numerically) introduce significant round-off error. To circumvent this problem, we make two assumptions that allow us to solve a simpler integral analytically then iterate to solve the resulting analytic equation for  $\Sigma$ . We note that if  $g^2$  is a constant,  $\Sigma$  is a function of only  $E$  (Ref. 6) and Eq. (3) can be integrated analytically. By replacing  $g^2(k-q)$  in Eq. (3) by a value independent of  $q$ ,  $g^2(k)$ , we still

preserve much of the structure of  $g^2$ . Our second simplification is to replace  $\Sigma(q, E - \hbar\omega)$  with  $\Sigma(k, E - \hbar\omega)$ . With these assumptions, Eq. (3) becomes

$$\Sigma_0(k, E) = g^2(k, E) \times \int dq \frac{1}{E - \hbar\omega - (\hbar^2 q^2 / 2m^*) - \Sigma_0(k, E - \hbar\omega)}, \quad (4)$$

which can be integrated analytically (for the sake of clarity, we have omitted a corresponding term for phonon absorption). Since  $g^2$  varies by several orders of magnitude over the  $q$  range of interest, it is of vital importance to choose a relevant value for  $g^2(k, E)$ . We define

$$g^2(k, E) = g^2(k - q^-(E)) + g^2(k + q^-(E)), \quad (5a)$$

where

$$q^-(E) = \frac{[2m^*(E - \hbar\omega)]^{1/2}}{\hbar}. \quad (5b)$$

The rationale behind this choice of  $g^2$  is the following: When we evaluate  $\Sigma(k, E)$  on the mass shell to obtain  $\Sigma(E)$ ,

$$\Sigma(E) = \Sigma\left(\frac{(2m^*E)^{1/2}}{\hbar}, E\right) = \Sigma(k, \varepsilon(k)), \quad (6)$$

then  $g^2(k, E)$  becomes equal to the classical coupling constant, which has the form  $g^2(q_p^+) + g^2(q_p^-)$  where  $q_p^\pm$  are the classical phonon wave vectors associated with forward and backward emission.

We solve Eq. (4) including absorption and emission over an energy range of  $-30$ – $180$  meV and use 150  $k$  values to obtain  $\Sigma_0(k, E)$  at room temperature. We can then interpolate between  $k$  values to obtain  $\Sigma_0(E)$ . Equation (4) converges after approximately 30 algebraic iterations; its output is then used as input to a numerical integration program which solves Eq. (3) exactly. The output from the analytic stage of the calculation is very close to the final result, therefore Eq. (3) converges after only two iterations.

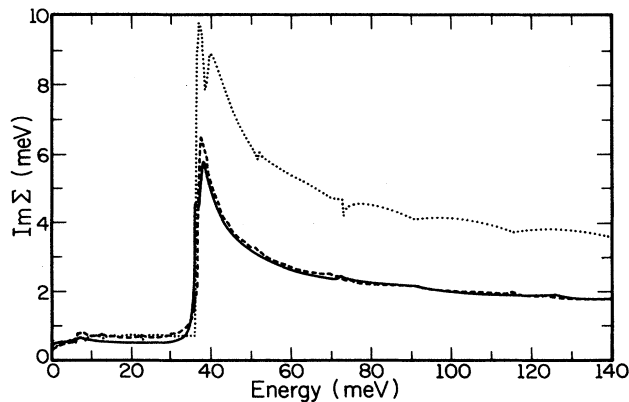


FIG. 1. Convergence of  $\text{Im}\Sigma(E)$ . Dotted line:  $\Sigma_0$  [the result of iterating Eq. (4)]. Dashed line:  $\Sigma_1$  [the result of inserting  $\Sigma_0$  into Eq. (3)]. Solid line:  $\Sigma$  [the result after two iterations on Eq. (3)].

In Fig. 1, we show the imaginary part of the self-energy along the classical energies  $E = \varepsilon(k)$ . The confinement conditions correspond to a square-well width of 135 Å and a triangular gate field of 120 kV/cm. (We have also computed  $\Sigma$  for a square-well width of 215 Å and a triangular gate field of 29 kV/cm.) The three curves shown are  $\Sigma_0$  [i.e., the result of iterating Eq. (4)],  $\Sigma_1$  [the result obtained by substituting  $\Sigma_0$  into the integrand of Eq. (3)], and  $\Sigma$  which is obtained by repeated iterations on Eq. (3). As can be seen from Fig. 1,  $\text{Im}\Sigma_0$  has the correct shape but exceeds the final result by about a factor of 2. The main discrepancies between  $\text{Im}\Sigma_0$  and  $\text{Im}\Sigma$  are due to the specific choice of  $g^2$  which is independent of  $q$  in  $\Sigma_0$ . In particular we use  $g^2 = 0$  below  $E = \hbar\omega$  because there is no way to define a classical phonon wave vector for emission in this region. This results in a sharp peak at  $E = \hbar\omega$  without broadening below the phonon energy.

In Figs. 2(a) and 2(b), we show the results for  $\text{Re}\Sigma$  and  $\text{Im}\Sigma$  plotted as functions of both  $k$  and  $E$ . Although we calculate  $\Sigma$  over an energy range of  $-30$ – $180$  meV and a  $k$  range from  $1 \times 10^5 \text{ cm}^{-1}$  to  $1 \times 10^8 \text{ cm}^{-1}$ , the plot covers a smaller area due to convergence problems near the borders. The energy axis ranges linearly from zero to 140 meV and the  $k$  axis varies logarithmically from  $1 \times 10^5 \text{ cm}^{-1}$  to  $2 \times 10^7 \text{ cm}^{-1}$ . The plots reveal two branches in

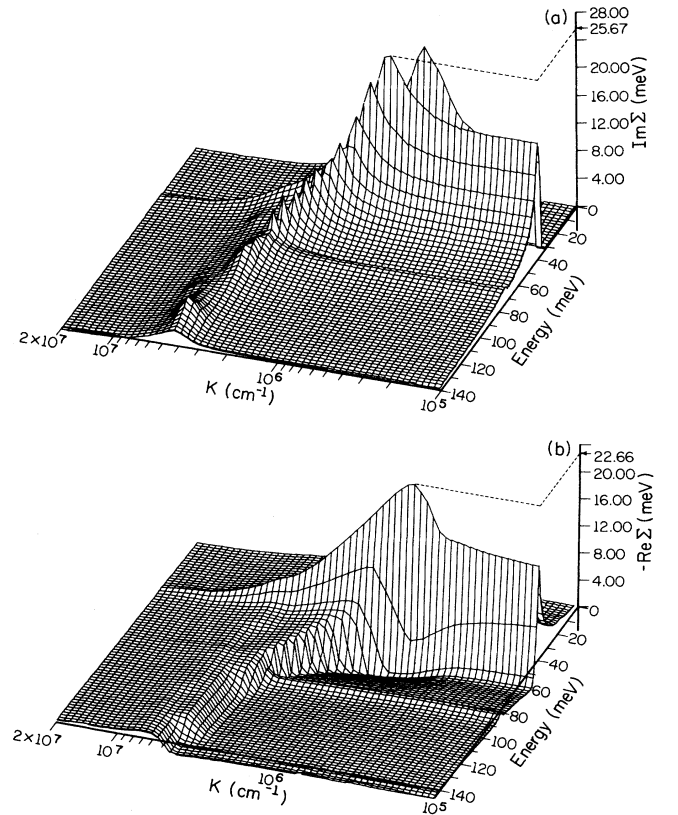


FIG. 2. Plot of  $\Sigma(k, E)$ . The energy axis ranges linearly from 0 to 140 meV and  $k$  ranges logarithmically from  $1 \times 10^5 \text{ cm}^{-1}$  to  $2 \times 10^7 \text{ cm}^{-1}$ . (a)  $\text{Im}\Sigma(k, E)$ ; (b)  $-\text{Re}\Sigma(k, E)$ . The phonon-like branch at  $E = \hbar\omega$  and the electronlike branch along  $E = \varepsilon(k)$  are visible in both plots.

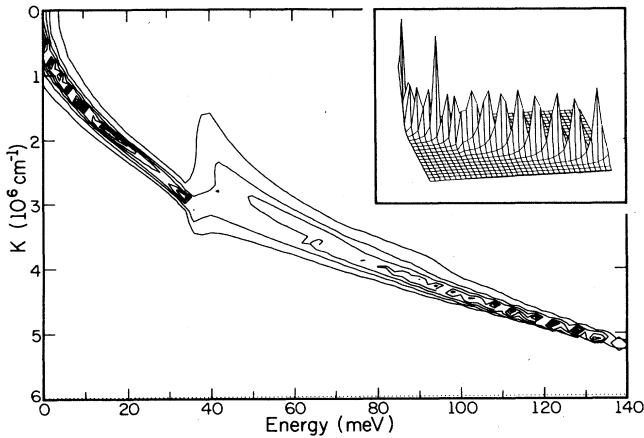


FIG. 3. Contour plot of the spectral density  $\rho(k, E)$ . Energy ranges linearly from 0 to 140 meV and  $k$  ranges linearly from 0 to  $6 \times 10^6 \text{ cm}^{-1}$ . The isolated peaks in  $\rho$  are due to the finite mesh employed in the plot. The inset shows a perspective view of  $\rho$  from the same viewing angle.

the self-energy, an electronlike branch and a phononlike branch. The sharp discontinuity just above  $E = \hbar\omega$  is particularly noticeable in  $\text{Re}\Sigma$  (for  $\text{Im}\Sigma$  the discontinuity is just below the emission threshold and not visible in Fig. 2) and corresponds to the phononlike branch. The electron branch starts near  $E = \hbar\omega$  and curves towards larger  $k$  and  $E$ , roughly following  $E = \varepsilon(k)$ . The jagged peaks in  $\text{Im}\Sigma$  along this branch are artifacts from the finite mesh and plotting package employed. The large peaks in both the real and imaginary parts occur at the phonon energy; however, they do not occur for the same  $k$  value nor do they lie along  $E = \varepsilon(k)$ . The peak in  $\text{Re}\Sigma$  corresponds to the minimum value of the denominator in Eq. (3) while  $g^2(k - q)$  reaches its peak value. From  $\text{Re}\Sigma$  we can see that there are states away from the classical regime but the lifetime of these states is short due to the large value of  $\text{Im}\Sigma$ . Further information above the excitation spectrum can be obtained from the spectral density  $\rho(k, E)$ ,

$$\rho(k, E) = \frac{-2\text{Im}\Sigma(k, E)}{[E - \varepsilon(k) - \text{Re}\Sigma]^2 + (\text{Im}\Sigma)^2}. \quad (7)$$

$\rho(k, E)$  is interpreted as the probability of the electron to have the energy  $E$  while in state  $k$ .<sup>7</sup> Figure 3 is a contour plot of  $\rho$  as a function of both  $k$  and  $E$ . It is obvious from the plot that  $\rho$  is negligible except along the classical dispersion  $E = \varepsilon(k)$ . Although there are states away from this dispersion, they have short lifetimes due to the high scattering rate. The electron can thus be described in classical (quasiparticle) terms.

In Fig. 4 we compare the self-consistent scattering rate  $2\text{Im}\Sigma/\hbar$ , with the rate obtained from Fermi's "golden rule" and a modified golden rule calculation where a broadening factor is used to "fudge" the quantum broadening effects in the final density of states. We per-

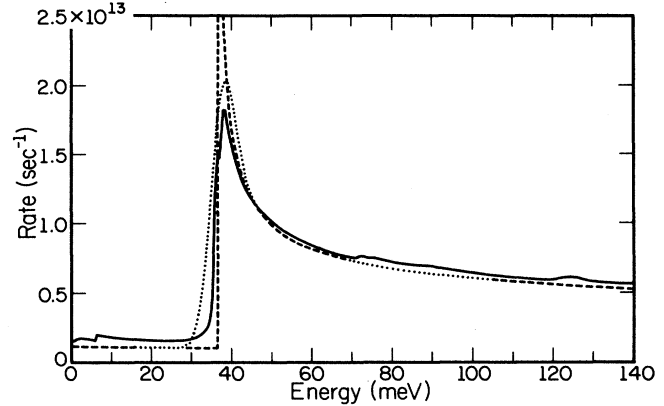


FIG. 4. Comparison of  $\Sigma$  with rates obtained from Fermi's "golden rule." Solid line:  $2\text{Im}\Sigma/\hbar$ . Dashed line: rates from Fermi's "golden rule." Dotted line: Fermi's "golden rule" using a density of states broadened by 2.5 meV.

form a convolution of the density of states with a Gaussian,<sup>8</sup>

$$D(E) = \frac{1}{\hbar\Gamma\sqrt{2\pi}} \left( \frac{m^*}{2} \right)^{1/2} \int_{-E}^{\infty} e^{-E'^2/2\Gamma^2} \frac{1}{\sqrt{E'+E}} dE', \quad (8)$$

where the amount of broadening  $\Gamma$  is set equal to 2.5 meV. As can be seen, both classical rates are good approximations away from the peak. The broadening smooths out the divergence in the scattering rate at the peak and allows for a much better fit there; it has a negligible effect on the rates away from the peak.

We have computed  $\Sigma$  and  $\rho$  and find that the spectral density function is essentially independent of the external potential for the different conditions considered. The self-energy is a function of the confinement, but its general shape remains unchanged. In addition, a good agreement can still be obtained between  $\text{Im}\Sigma$  and the scattering rate from Fermi's "golden rule" by use of a 2.5 meV broadening factor.

In conclusion, we have calculated the self-energy  $\Sigma(k, E)$  for the electron-phonon interaction in 1D systems. Although  $\Sigma$  has a phononlike branch and shows significant features away from the classical dispersion, the spectral function is essentially zero away from the noninteraction energies which implies that the system can be described adequately in terms of a quasiparticle model. We have compared  $\text{Im}\Sigma$  to the rates from Fermi's "golden rule" and find the semiclassical result to be an excellent approximation away from the peak; a constant broadening factor in the final density of states accounts for the general feature of quantum effects in the scattering rates at the peak.

We thank Karl Hess for helpful discussions. This work was supported by the National Science Foundation under Grant No. NSF-ECS-85-10209, and the Joint Services Electronics Program.

- \*Current address: Department of Physics and Astronomy, University of Oklahoma, 440 West Brooks, Room 131, NH, Norman, OK 73019.
- <sup>1</sup>K. Ismail, D. Antoniadis, and H. Smith, *Appl. Phys. Lett.* **54**, 1130 (1989).
- <sup>2</sup>S. Datta and M. McLennan, in *Nanostructure Physics and Fabrication*, edited by M. A. Reed and W. P. Kirk (Academic, Boston, 1989).
- <sup>3</sup>E. M. Conwell, *High Field Transport in Semiconductors* (Academic, New York, 1967).
- <sup>4</sup>D. Pines, in *Polarons and Excitons*, edited by C. G. Kuper and G. D. Whitfield (Plenum, New York, 1963), p. 155.
- <sup>5</sup>K. Kim, B. Mason, and K. Hess, *Phys. Rev. B* **36**, 6547 (1987).
- <sup>6</sup>Y. C. Chang, D.Z.-Y. Ting, J. Y. Tang, and K. Hess, *Appl. Phys. Lett.* **42**, 76 (1983).
- <sup>7</sup>G. D. Mahan, *Many-Particle Physics* (Plenum, New York, 1981).
- <sup>8</sup>S. Briggs and J. P. Leburton, *Phys. Rev. B* **38**, 8163 (1988) [in the reference, Eq. (5) should show the correct limits of integration, not  $-\infty$  to  $+\infty$ ].